

A Lorentz covariant model of string fragmentation

Jade Abidi

Student ID: 31461964

A thesis submitted for the degree of **Bachelor of Science (Honours)**

November 2025

School of Physics and Astronomy
Monash University

Supervisor: Peter Skands

Abstract

Monte Carlo event generators are extensively used to simulate high-energy particle-collision events. For analytically intractable aspects, they rely on phenomenological models. The so-called Lund model describes the non-perturbative hadronisation process as the fragmentation of a classical string with constant tension. Lorentz covariance then implies the self-similarity of this fragmentation process along the string. The current formulaion of the Lund model, used in the PYTHIA generator, violates this property in terms of both kinematic distributions and hadronic chemistry. We introduce an additional tunable parameter and a new algorithm for string fragmentation that improve or resolve these issues, albeit with some limitations.

Contents

1	Introduction	2
2	QCD, the Lund Model, and PYTHIA	4
2.1	Quantum Chromodynamics and Collider Physics	4
2.2	Monte Carlo Event Generators and PYTHIA	9
2.3	The Lund String Model	10
3	String Fragmentation in PYTHIA	12
3.1	The PYTHIA Fragmentation Algorithm	12
3.2	The Joining Step	13
3.3	Performance of the Current finalTwo Procedure	14
4	Tuning Lightcone Scaling in PYTHIA	15
4.1	Restoring Lightcone Scaling by Tuning Parameters	15
4.2	The probRevertBreak parameter	15
4.3	Limitations	15
5	The Accordion Algorithm for String Fragmentation	17
5.1	The Accordion Algorithm	17
5.2	Pseudocode	17
5.3	Results	17
5.4	Limitations	17
6	Summary and Outlook	19

Chapter 1

Introduction

The field of particle physics investigates the most fundamental particles and interactions in nature. It naturally evolved from nuclear and atomic physics in the early 20th century as technological and scientific knowledge allowed scientists to probe matter at higher energies and smaller length scales [1,2]. The physical theory underpinning particle physics developed out of quantum field theory, culminating in the Standard Model of particle physics which was formalised in the 1980s. The Standard Model unifies three of the four fundamental forces of nature (electromagnetism, the weak force, and the strong force) into a single theory, and predicted the existence of the Higgs boson well before its historic discovery at the Large Hadron Collider (LHC) in 2012 [3,4].

The interactions investigated in particle-physics experiments occur at high energies, with low probabilities. Particle colliders, such as the LHC, are designed specifically to enable such experiments by accelerating charged particles, usually electrons or protons (and their antiparticles), to speeds up to 99.9999% of the speed of light. Most modern particle colliders are circular, and use high voltages and strong magnetic fields to accelerate particles and keep them within a thin beamline. The particle beams are then made to collide millions of times every second at interaction points, around which bespoke detector systems collect data on the final state [1,5,6].

For comparison against this data, it is very useful to be able to generate ensembles of large numbers of events based on physical models and assumptions. Because the physics involved is so complex and often lacks an analytic solution, Monte Carlo event generators such as PYTHIA provide a way to sample the phase space efficiently [1,7–9]. Powerful factorisation theorems allow for the various processes that occur at different energy scales to be modelled independently of each other, which greatly simplifies the problem [9,10]. The focus of this project is the process of hadronisation, in which partons (quarks and gluons) form hadronic bound states. This occurs at momentum transfer scales below the confinement energy of $\Lambda_{\text{QCD}} \sim 0.2 \text{ GeV}$ [9].

Due to asymptotic freedom, the coupling constant of the strong force becomes very large for momentum transfers in this range [11], and therefore the physics of hadronisation cannot be calculated perturbatively. Non-perturbative quantum chromodynamics has not yet been analytically solved, and numerical methods such as lattice QCD have limitations that render them inapplicable to hadronisation [12]. Instead, PYTHIA uses the Lund string model as a description of hadronisation, which is a phenomenological theory (and is not derivable from first principles) [7,13].

In the Lund string model, the strong field between a quark and antiquark is modelled as a string with constant tension $\kappa \sim 0.9 \text{ GeV}$ per femtometre, as measured in lattice

QCD simulations [9, 14]. At separation distances of $\gtrsim 1\text{ fm}$, there is enough potential energy stored in the string for it to ‘‘break’’, forming a new quark-antiquark pair. This leaves two quark-antiquark string subsystems, which proceed to break in the same manner as the original system, giving rise to a recursive self-similar process resulting in a set of outgoing bound states of quarks [7, 9, 13, 15].

This self-similarity of the fragmentation process along the string is one of the most important properties of the Lund string model. The string breaks are all spacelike separated and hence cannot causally influence each other, and the tension along the string is constant and invariant under longitudinal boosts. It therefore follows that, away from the endpoints of the string, all fragmentation observables (like the number or species of hadrons produced from a region of the string) must be invariant under Lorentz boosts (or equivalently, rapidity translations) along the string axis. This means that distributions such as hadron density per unit rapidity should be flat except for endpoint effects (denoted the ‘‘rapidity plateau’’). It also implies that, if considered iteratively, the process by which each string subsystem is fragmented must be scale invariant [7, 13, 15].

Despite the importance of the Lorentz covariance of string fragmentation in the Lund model, current simulations in PYTHIA reveal that this property is quite badly broken. Since the release of PYTHIA 8.0, the rapidity plateau has exhibited a significant dip in the central region. Initial investigations revealed this to be a consequence of the hadronisation algorithm used in PYTHIA, where the final two hadrons have kinematics forced by energy-momentum conservation and the mass-shell relation. In the Monash tune of PYTHIA 8.3, the rapidity spacing between these final two hadrons is larger than the typical rapidity spacing. This, combined with the non-uniformity of location of the joining step along the string, gives rise to this central rapidity dip. Furthermore, the `finalTwo` procedure that generates these hadrons fails about 50% of the time, introducing bias that skews the species makeup of these final two hadrons.

PYTHIA offers three tunable parameters that adjust the behaviour of this procedure — `stopMass`, `stopNewFlav`, and `stopSmear`. Prior to this project, it was believed that these parameters could be tuned to give a flat rapidity plateau, and would not need to be retuned when other fragmentation parameters change [7, 16]. This is not the case for the Monash tune, where it is impossible to achieve a flat plateau with these parameters without significantly worsening the failure rate of `finalTwo`.

In this thesis, chapter 2 provides a review of the theoretical background of quantum chromodynamics, PYTHIA, and the Lund string model. In chapter 3, the current behaviour of the PYTHIA hadronisation algorithm is analysed in more detail, and the various problems are described and explained. In chapter 4, the tuning of the `finalTwo` parameters is discussed. An additional tunable parameter `revertFinalBreak` is presented which provides an additional dimension of parameter space and allows for a flatter rapidity plateau to be obtained without as much of an impact on the failure rate. Finally, in chapter 5, an alternative algorithm for hadronisation in PYTHIA is developed, called the accordion join, which achieves an approximately flat rapidity plateau for any tune, and fails more than a hundred times less frequently.

Chapter 2

QCD, the Lund Model, and PYTHIA

2.1 Quantum Chromodynamics and Collider Physics

Before introducing PYTHIA and the Lund string model, we first provide an overview of the theoretical models and experimental techniques used in particle physics, with a focus on quantum chromodynamics.

The field of particle physics developed out of the study of atomic and nuclear physics in the early 20th century. Experiments like the discovery of the nucleus in 1911 [17] or the neutron in 1932 [18] paved the way for the development of more advanced technologies such as particle accelerators and colliders. The high centre-of-mass energies reached in these experiments allowed for the discovery of a slew of particles in the 1950s and 1960s, dubbed the “particle zoo” [2]. Alongside these experiments, the theoretical success of quantum mechanics inspired the quantisation of the electromagnetic field in the original formulation of quantum field theory (QFT) and quantum electrodynamics (QED) by Dirac, who notably predicted the existence of antimatter a number of years before its discovery [19, 20]. QED was later unified with a description of the weak force (responsible for phenomena like beta decay) into electroweak theory, a Yang-Mills gauge theory consisting of a local $U(1) \times SU(2)$ gauge symmetry [1, 21].

At the same time, quantum chromodynamics (QCD) emerged, describing the variety of particles discovered in the “particle zoo” as composed of more fundamental subatomic particles — quarks and gluons. Initial models like the Eightfold Way classified these various strongly interacting particles as hadrons emerging from a $SU(3)$ flavour symmetry between three quark flavours [22, 23], as shown in Figure 2.1. These flavours were later denoted the up (u), down (d), and strange (s) quarks, and three more (charm, beauty, and top) were eventually found. Hadrons were classified into two groups — mesons, which are bosonic bound states consisting of a quark and an antiquark, and baryons, which are fermions consisting of three quarks or antiquarks. The experimental reality of these quarks outside of phenomenology was confirmed by deep inelastic scattering experiments, which showed pointlike constituents within the proton, called partons [6, 21].

It was later found that these partons come in two types — the spin $\frac{1}{2}$ quark, and the spin 1 gluon [1]. The existence of the gluon was confirmed in the JADE experiment [24], which was notably one of the first uses of Monte Carlo event generators in the analysis of experimental data. In addition to their electromagnetic charge, quarks and gluons also carry colour charge, which has three components labelled red, green, and blue (with cyan,

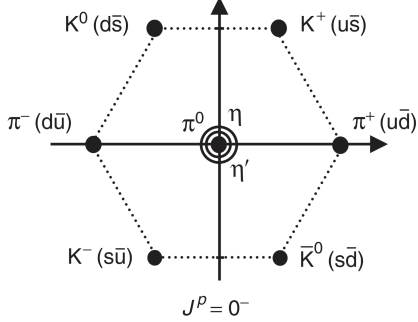


Figure 2.1: A visual depiction of the pseudoscalar mesons in the Eightfold Way, which form an octet and a singlet in $SU(3)$ flavour space [22, 23]. The horizontal axis represents I_3 , an isospin component, and the vertical axis represents Y , the hypercharge, both of which are quantum numbers arising from the $SU(3)$ flavour symmetry. Figure taken from [21].

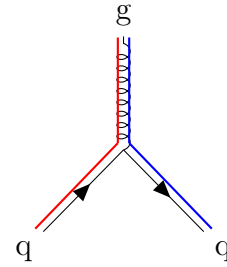


Figure 2.2: An illustration of a qqq vertex in QCD, showing the colour flow. The incoming and outgoing quarks have one colour, while the gluon has two (a colour and anticolour).

magenta, and yellow as their anticolour opposites) [1, 21].

In the 1970s, a formal theory of QCD based on a $SU(3)$ gauge symmetry was developed, and by 1980, the Standard Model was formalised, which unified the electromagnetic, weak, and strong forces into a single unified gauge theory with three generations of fermions (6 quarks and 6 leptons). Collider experiments throughout the following years continued to confirm predictions of the Standard Model, and it has since become our most successful and fundamental model of physical reality [3, 21].

A full theoretical description of QFT and QCD is outside the scope of this review, and we will only provide a brief summary in order to establish the necessary theoretical background. The reader is directed to the textbook by Peskin and Schroeder [25] for a general overview of quantum field theory, or the textbook by Ellis, Stirling, and Webber [6] for closer detail on quantum chromodynamics or collider physics.

Quantum field theories model particles as excitations of underlying quantised fields, which are operator-valued at every point in space and time. Particles interact via the exchange of bosons as virtual particles, and in this way the concept of a “force” is reduced to an allowed interaction between particles. As in quantum mechanics, these particles can be more or less localised in coordinate or momentum space, with these two uncertainties linked by Heisenberg’s relation

$$\Delta x \Delta p_x \geq \frac{\hbar}{2}. \quad (2.1)$$

Typically, in particle physics, particles are described as entirely delocalised plane waves with precisely defined energies and momenta. This is justified because the length scales involved in particle collisions are much smaller than typical De Broglie wavelengths, and in this limit the physical extent of the particle’s wave packet is not relevant.

The physical laws governing these quantised fields are captured in the Lagrangian, and can be derived via the Euler-Lagrange equations. In a gauge theory, these Lagrangians are derived to obey underlying local gauge symmetries. QCD is based on a local $SU(3)$ gauge symmetry, which implies that the wavefunction must carry three additional degrees of freedom representing the colour charge. The three fundamental colour states

corresponding to red, green, and blue are

$$r = \begin{pmatrix} 1 \\ 0 \\ 0 \end{pmatrix}, \quad g = \begin{pmatrix} 0 \\ 1 \\ 0 \end{pmatrix}, \quad \text{and} \quad b = \begin{pmatrix} 0 \\ 0 \\ 1 \end{pmatrix}. \quad (2.2)$$

A local SU(3) gauge transformation is a rotation of states in colour space, where the axis and amount of rotation can vary throughout time and space. The Noether invariant corresponding to this symmetry is colour charge, which is a conserved quantity in QCD.

In QCD, the strong interaction is mediated by the eight gluons, corresponding to the eight generators of the SU(3) group. Unlike quarks, gluons carry a combination of colour charge and anticharge. Since quarks are the only fermions that carry colour charge in the Standard Model, only quarks can couple to gluons. The Lagrangian density describing QCD is given by

$$\mathcal{L} = \bar{\psi}_q^i (i\gamma^\mu) (D_\mu)_{ij} \psi_q^j - m_q \bar{\psi}_q^i \psi_{qi} - \frac{1}{4} F_{\mu\nu}^\alpha F^{\alpha\mu\nu}. \quad (2.3)$$

Here, the first term describes the kinetic energy of quarks and their interaction with gluons, the second term endows quarks with their mass, and the third term allows for gluon-gluon interactions. Figure 2.2 shows how colour flows through a quark-gluon Feynman interaction vertex. Because the generators of SU(3) do not commute, QCD is a non-Abelian gauge theory and therefore gluon-gluon interactions are also possible. This is in contrast to quantum electrodynamics, where there is no photon-photon coupling term in the Lagrangian [1, 6, 21].

An important property of QCD is confinement. The quarks and gluons that make up hadrons have never been observed on their own as free particles. In nature, they seem to always be confined to hadronic bound states, and cannot be separated beyond the typical hadron size of ~ 1 fm. Confinement has not been mathematically proven—indeed, its proof is one of the Millennium Prize Problems (a consequence of the Yang-Mills existence and mass gap). However, it can still be understood as a consequence of the running coupling of QCD. Figure 2.3 shows how the coupling constant (describing the strength of the strong interaction) decreases with the energy scale of the interaction [1]. As such, at short distances (and high energies) the strong interaction is weak, but at longer distance the strong interaction becomes strong enough to forbid the separation of quarks and gluons. This phenomenon is known as asymptotic freedom [26].

The strong potential between quarks and antiquarks is given by the Cornell potential,

$$V(r) = -\frac{4}{3} \frac{\alpha_s}{r} + \kappa r, \quad (2.4)$$

which combines a short-distance Coulomb potential with a stronger, longer-distance linear potential. Here, α_s is the strong coupling constant, and κ is a constant measured to be approximately 1 GeV fm^{-1} . Figure 2.4 shows lattice QCD calculations of the strong potential between a $q\bar{q}$ pair, exhibiting Coulombic behaviour at short distances and becoming linear for longer distances. Because QCD allows for gluon-gluon interactions, the linear potential can be understood as a result of the self-attraction of strong field lines, which compresses the field into a flux tube with constant tension. It is this linear potential that gives rise to the confinement distance of approximately 1 fm, at which it is energetically favourable for the strong field to break into a new quark-antiquark pair, forming a new hadron. This “string-breaking” model of hadron formation is the basis for the Lund string model, described further in section 2.3.

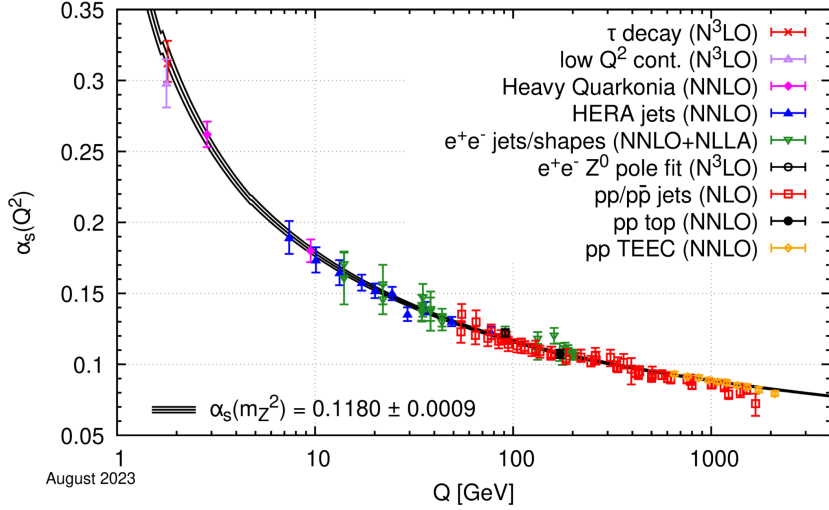


Figure 2.3: The running of the QCD coupling constant $\alpha_S(Q^2)$ with respect to the energy scale Q . The PDG average is shown as a solid line alongside data points from numerous experiments. The asymptotic freedom of QCD is evident from how the coupling constant is sufficiently small for perturbation theory at large values of Q , but becomes prohibitively large for smaller values of Q . Figure taken from [1].

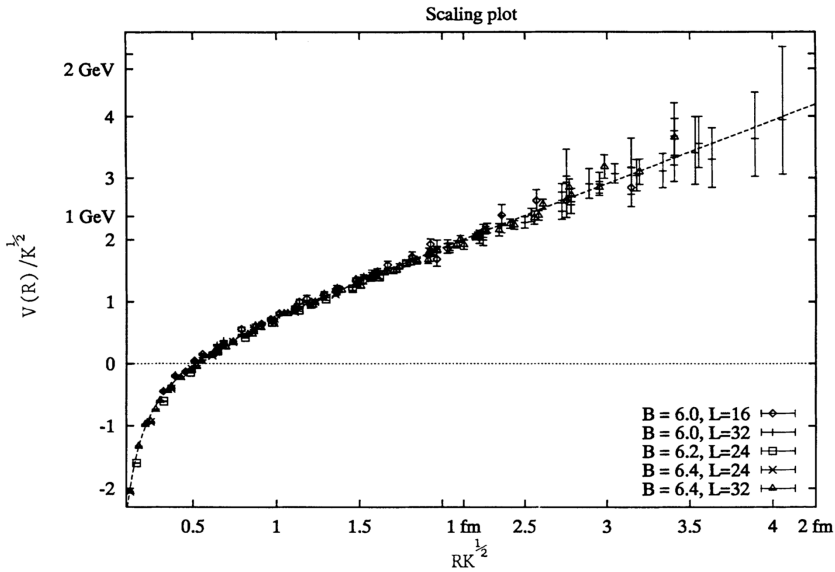


Figure 2.4: The potential between a quark and antiquark as a function of distance. Data points are obtained from lattice QCD simulations [14], and the dotted line shows the Cornell potential as defined in equation (2.4). Except for at short distances, the potential is approximately linear, motivating the treatment of the colour field as a classical string with constant tension. Figure taken from [14].

As mentioned in the introduction, experiments in particle physics require very high centre-of-mass energies for the interactions under observation to be kinematically allowed. If two particle beams have energies E_1 and E_2 , then the resulting relativistic centre-of-mass (CM) energy is given by

$$E_{\text{CM}} \approx 2\sqrt{E_1 E_2}, \quad (2.5)$$

which reduces to $E_{\text{CM}} = 2E_b$ if the two beam energies are the same, which is common in modern colliders. The Large Hadron Collider has achieved CM energies up to 13.6 TeV.

Another important property of particle colliders is luminosity. While the beam and centre-of-mass energies describe the energies achieved by individual particles in the collider, the luminosity quantifies the flux of particles in the beam. Luminosities in modern colliders are quite large; the most recent LHC experiments have luminosities around $5 \times 10^{34} \text{ cm}^{-2} \text{ s}^{-1}$.

The “probability” of a given interaction occurring is quantified by the cross section σ . The cross section has units of area, but typical cross sections are so small that the standard unit is barns, where 1 barn is equal to $1 \times 10^{-28} \text{ m}^{-2}$. Despite not actually representing a physical area, the cross section generalises the notion of the area of a target representing its probability of being struck by an incoming particle. The variation of the interaction probability over the values of a variable, such as the solid angle Ω , is often expressed using the differential cross section $d\sigma/d\Omega$, which is related to the overall cross section by

$$\sigma = \int \frac{d\sigma}{d\Omega} d\Omega. \quad (2.6)$$

Here, Ω can be replaced with any number of variables, such as the Mandelstam variable s which quantifies the CM energy of the collision. If $\mathcal{L}(t)$ is the instantaneous luminosity of a particle beam, then the expected number of events with cross section σ is

$$N = \sigma \int \mathcal{L}(t) dt. \quad (2.7)$$

In this way, the cross section solely represents the underlying physics of an interaction, with the specific experimental collider setup factorised out.

The most important particle colliders for experimental QCD are typically proton-proton (pp) colliders, also called hadron colliders. The first hadron collider was the Intersecting Storage Rings (ISR) at CERN, which were operational from 1971, with a centre-of-mass energy of 62 GeV [1, 27, 28]. It was succeeded by the Tevatron which, as suggested by its name, reached centre-of-mass energies of 1 TeV [29]. Notable discoveries such as that of the top quark were made by the Tevatron [30, 31]. Currently, the largest hadron collider is the creatively named Large Hadron Collider (LHC) described above, which was operational from 2008 and is responsible for the monumental discovery of the Higgs boson in 2012 [4, 32]. A photo of the Compact Muon Solenoid (CMS) detector, one of the particle detectors in the LHC, is shown in Figure 2.5.

Detectors are only able to measure the final state of an event, and ultimately output a list of the types, masses, and four-momenta of the outgoing particles. For high-luminosity colliders like the LHC, many billions of these event records are recorded. For many theoretical aspects of QCD, it is only possible to compare experimental data to theory by using Monte Carlo techniques to generate ensembles of events based on theoretical assumptions. As mentioned earlier, the discovery of the gluon in the JADE experiment utilised the JETSET generator. The next section outlines the functionality of these event generators, with a focus on PYTHIA, the modern successor to JETSET.

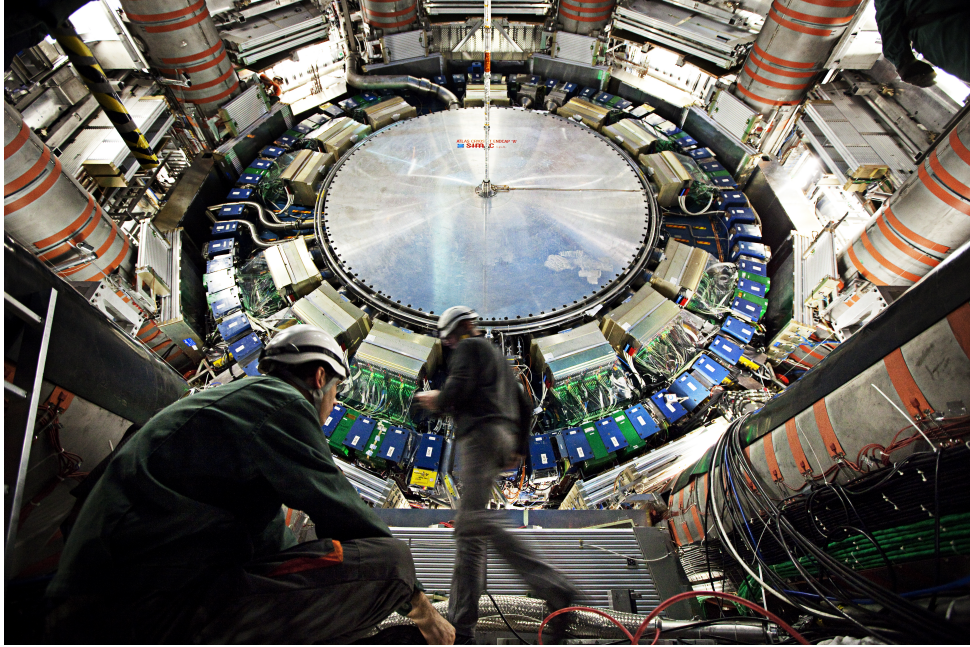


Figure 2.5: The ATLAS detector, the largest of the particle detectors at the LHC. It was involved in the discovery of the Higgs boson in 2012 [4]. The particle beams are contained within the thin tube visible at the top centre of the image, and the rest of the structure contains detectors that measure the energy and momentum of final state particles. Figure from [33].

2.2 Monte Carlo Event Generators and PYTHIA

1. Explain what a Monte Carlo event generator is and what role it plays in particle physics.
2. Explain why Monte Carlo simulation is necessary to generate events, including the difficulties with non-perturbative QCD and numerical calculations like lattice QCD.
3. Sketch the history of Monte Carlo event generators, including JETSET, PYTHIA, HERWIG, and more. Outline differences between these generators.
4. Elaborate on the history and features of PYTHIA. Include a few potential uses.
5. Explain how an event is generated in PYTHIA. Include a high-level mathematical formulation of the hard scattering, parton shower, hadronisation, and decays. Introduce and explain why factorisation allows us to consider different energy scales of event generation independently of each other.
6. Figure: That big cool looking one from the PYTHIA documentation.
7. Elaborate on the hadronisation process. Emphasise the necessity of phenomenological models due to the non-perturbative physics involved. Signpost the Lund model.
8. Explain the necessity of tuning and how this process works.

2.3 The Lund String Model

1. Introduce the history and development of the Lund string model. Outline a high level of how it models hadronisation using string breaks.
2. Figure: Hadronisation according to the Lund model.
3. Explain how the Lund model describes the strong colour field as a flux tube with linear potential.
4. Explain the experimental and phenomenological justification for the Lund model. Include lattice QCD simulations of the string tension, and the existence of ggg and gggg interaction vertices in QCD as a reason for the flux tube behaviour.
5. Figure: The electric field vs. the colour field
6. Introduce the yo-yo mode and explain how it is a model for hadrons in the Lund model. Introduce diquarks.
7. Figure: Spacetime diagram of the yo-yo mode.
8. Introduce rapidity and lightcone momenta.
9. Figure: Rapidity vs velocity.
10. Explain how string fragmentation works in the Lund model. Establish that the fragmentation process is fully specified by z fractions. Introduce the fragmentation functions and lightcone scaling, as well as the Schwinger mechanism.
11. Figure: Spacetime diagram of string fragmentation.
12. Briefly introduce gluon kinks and more complex string topologies.
13. Figure: String topologies in the Lund model.
14. Emphasise how the string fragmentation properties are asymptotic in the limit where energy-momentum conservation is not a consideration.

Chapter 3

String Fragmentation in PYTHIA

3.1 The PYTHIA Fragmentation Algorithm

1. Outline what a successful implementation of the Lund model would achieve. Note how the problem is somewhat undefined in terms of energy-momentum conservation.
2. Explain the current hadronisation algorithm in PYTHIA.
3. Outline the Eden paper and how the PYTHIA manuals describe the joining step and energy-momentum conservation in PYTHIA and the Lund model.
4. Pseudocode: The PYTHIA hadronisation algorithm.

Having established the theoretical basis of the Lund string model for hadronisation, we can now describe how the hadronisation process is algorithmically implemented in PYTHIA. We begin by outlining what a “successful” implementation of the Lund string model would achieve. As mentioned in section 2.3, the 1+1-dimensional kinematics (((TODO: Maybe rephrase this?))) of string fragmentation in a single event that produces N hadrons are completely specified by a set of N absolute lightcone momentum fractions $\{z_{\text{abs},i}^+\}$, where we are considering fragmentation right-to-left (but could just as well consider it left-to-right).

To conserve energy and momentum, these lightcone momentum fractions must add to unity, that is,

$$\sum_{i=1}^N z_{\text{abs},i}^+ = 1. \quad (3.1)$$

The area law and lightcone scaling properties of the Lund string model require that the relative lightcone momentum fractions $\{z_i^+\}$ of a single event (as defined in section 2.3) are all drawn from a given fragmentation function $f(z)$ — specifically, the Lund symmetric fragmentation function specified in equation (((insert equation here))).

Also established in section 2.3 is the fact that the quarks produced along the string must have masses m_q and transverse momenta $p_{\perp,q}$ drawn from a distribution $\text{Pr}(m_q^2, p_{\perp,q}^2)$ with a Gaussian suppression, as in equation (((insert equation here))). The resulting hadrons formed from these quarks (and antiquarks) must have masses and transverse momenta distributed accordingly.

(((TODO: Is this a good description? Is this necessary? What about the distribution of N ?)))

The actual implementation of string fragmentation in PYTHIA is given by the high-level pseudocode in (((link))). Here, we are considering the simplest fragmentation process where a quark q_0 and antiquark \bar{q}_0 move in opposite directions along the z -axis with centre-of-mass energy E_{CM} . An actual event in PYTHIA will contain many such processes between different partons produced in the parton shower, and will also require the consideration of gluon kinks along the strings. (((TODO, elaborate, make less vague))) However, as we will see, lightcone scaling is entirely violated in PYTHIA even in this minimal situation, and as such the rest of this thesis will be limited to simple $q\bar{q}$ hadronisation.

Algorithm 1 The default PYTHIA 8.3 algorithm for $q\bar{q}$ hadronisation

```

procedure FRAGMENT( $E_{\text{CM}}$ ,  $\text{flav}(q_0)$ ,  $\text{flav}(\bar{q}_0)$ )
    initialise event record event
     $i \leftarrow 1$ 
     $p_x(q_0) \leftarrow 0.0$ 
     $p_y(q_0) \leftarrow 0.0$ 
     $p_x(\bar{q}_0) \leftarrow 0.0$ 
     $p_y(\bar{q}_0) \leftarrow 0.0$ 
    loop
        fromPos  $\leftarrow$  true or false with equal probability
         $\text{flav}(q_i) \leftarrow$  flavour according to Gaussian suppression ((equation)) and PYTHIA
        weights
         $\text{flav}(\bar{q}_i) \leftarrow$  antiflavour of  $\text{flav}(q_i)$ 
         $p_x(q_i) \leftarrow$  transverse momentum according to Gaussian suppression ((equation))
         $p_x(\bar{q}_i) \leftarrow -p_x(q_i)$ 
         $p_y(q_i) \leftarrow$  transverse momentum according to Gaussian suppression ((equation))
         $p_y(\bar{q}_i) \leftarrow -p_y(q_i)$   $\triangleright$  String break done.
        if fromPos then
             $\text{event}[i].id \leftarrow$  hadron selected from combination of  $\text{flav}(q_{i-1})$  and  $\text{flav}(\bar{q}_i)$ 
             $\text{event}[i].m \leftarrow$  mass selected according to Breit-Wigner distribution
             $\text{event}[i].p_x \leftarrow p_x(q_{i-1}) + p_x(\bar{q}_i)$ 
             $\text{event}[i].p_y \leftarrow p_y(q_{i-1}) + p_y(\bar{q}_i)$ 
        else
        end if
    end loop
end procedure

```

3.2 The Joining Step

1. Pseudocode: The PYTHIA finalTwo
2. Explain in close detail how the finalTwo joining step works in PYTHIA.
3. Explain the stopMass, stopNewFlav, and stopSmear parameters work.
4. Note the inherent violation of lightcone scaling. Explain how the manual and documentation claim this is resolved.

3.3 Performance of the Current finalTwo Procedure

1. Figure: dN/dy distributions in PYTHIA 8.3 vs 8.0 vs 6, for varying string lengths.
2. Explain how bad the problem is with rapidity distributions. Also mention the tune loading bug.
3. Explain why this happens in terms of the stopMass parameter, rapidity spacing, and fragmentation functions, as well as the non-uniformity of the joining step rank.
4. Figure: W_{rem} plots for the joining step across different versions, as well as rapidity spacing plots.
5. Data: Example ratio differences and SSE of hadronic chemistry in the joining step, PYTHIA 6 vs 8.
6. Explain the bias introduced by the finalTwo failure rate and how this leads to an anomalous hadronic chemistry.

Chapter 4

Tuning Lightcone Scaling in PYTHIA

4.1 Restoring Lightcone Scaling by Tuning Parameters

1. Explain the necessity of tuning the joining step, in contradiction to what was asserted by the manual.
2. Explain the tradeoff between hadronic chemistry and kinematics of the joining step hadrons, and the difficulty in tuning for both with only one degree of freedom.
3. Data: Rapidity plateaus, SSEs of rapidity plateaus and hadronic chemistry across different joining step parameters and tunes.
4. Figure: Plots of SSEs across parameters and tunes.

4.2 The probRevertBreak parameter

1. Introduce the probRevertBreak parameter and the pseudocode. Explain how the algorithm works and what is changed. Include formulas for conditional spin switching.
2. Explain how the probRevertBreak parameter reduces bias and improves hadronic chemistry, as well as providing more freedom to tune the joining step.
3. Show results (SSEs and rapidity plateaus) of probRevertBreak and the possibility for improvement.

4.3 Limitations

1. Explain the limitations of this set of parameters, showing plots of rapidity differences at the joining step vs everywhere else.
2. Re-emphasise how issues like anomalous hadronic chemistry and the rapidity plateau are not fixed.

3. Note the issues with finalTwo failing. Cite a few papers that are affected by this.

Chapter 5

The Accordion Algorithm for String Fragmentation

5.1 The Accordion Algorithm

1. Motivate the concept behind the accordion algorithm. Re-emphasise the self-similarity and causal independence of breakup vertices.
2. Establish the goals of the algorithm - a flat rapidity plateau, correct hadronic chemistry, and a lower failure rate.
3. Explain how the algorithm works. Derive equations relating rapidity spacing and z fractions. Explain the accordion rescaling and why numerical solution is required.
4. Elaborate on limitations of the accordion rescaling, including the shaky Lorentz covariance and effect on fragmentation functions. Explain why fragmentation functions may not matter.

5.2 Pseudocode

1. Show and explain pseudocode of the accordion algorithm.

5.3 Results

1. Show off!

5.4 Limitations

1. Be honest. But in a nice way.
2. Not implemented for popcorn model.
3. Needs to be expanded to gluon kinks and string topologies - not clear how this might work.
4. Necessity of tuning stopMass.

5. Need more investigation into correlations and fragmentation functions.

Chapter 6

Summary and Outlook

1. Summarise the achievements and results, re-establishing their context in the broader field.
2. Establish further avenues of investigation, including: expanding the scope of the algorithm, improving the rescaling step, improving the rapidity spacing sampling, investigating time complexity and performance, investigating the effects of the rapidity dip in other findings and papers

Bibliography

- [1] Particle Data Group, *Review of particle physics*, *Phys. Rev. D* **110** (2024) 030001.
- [2] F. Gross et al., *50 Years of Quantum Chromodynamics*, *Eur. Phys. J. C* **83** (2023) 1125 [[2212.11107](#)].
- [3] M.D. Schwartz, *Quantum field theory and the standard model*, Cambridge University Press, New York (2014), [10.1017/9781139540940](#).
- [4] A. Collaboration, *Observation of a new particle in the search for the Standard Model Higgs boson with the ATLAS detector at the LHC*, *Phys. Lett. B* **716** (2012) 1.
- [5] L. Evans and P. Bryant, *LHC machine*, *JINST* **3** (2008) S08001.
- [6] R.K. Ellis, W.J. Stirling and B.R. Webber, *QCD and collider physics*, Cambridge University Press, Cambridge (1996), [10.1017/CBO9780511628788](#).
- [7] C. Bierlich et al., *A comprehensive guide to the physics and usage of PYTHIA 8.3*, *SciPost Phys. Codeb.* **2022** (2022) 8 [[2203.11601](#)].
- [8] A. Buckley et al., *General-purpose event generators for LHC physics*, *Phys. Rept.* **504** (2011) 145 [[1101.2599](#)].
- [9] P. Skands, *Introduction to QCD*, in *Theoretical Advanced Study Institute in Elementary Particle Physics: Searching for New Physics at Small and Large Scales*, pp. 341–420, 2013, DOI [[1207.2389](#)].
- [10] J.C. Collins and D.E. Soper, *Parton Distribution and Decay Functions*, *Nucl. Phys. B* **194** (1982) 445.
- [11] D.J. Gross and F. Wilczek, *Asymptotically Free Gauge Theories - I*, *Phys. Rev. D* **8** (1973) 3633.
- [12] G.P. Salam, *Elements of QCD for hadron colliders*, in *2009 European School of High-Energy Physics*, 11, 2010 [[1011.5131](#)].
- [13] B. Andersson, G. Gustafson, G. Ingelman and T. Sjostrand, *Parton Fragmentation and String Dynamics*, *Phys. Rept.* **97** (1983) 31.
- [14] G.S. Bali and K. Schilling, *Static quark - anti-quark potential: Scaling behavior and finite size effects in SU(3) lattice gauge theory*, *Phys. Rev. D* **46** (1992) 2636.
- [15] B. Andersson, *The Lund Model*, vol. 7, Cambridge University Press (1998), [10.1017/9781009401296](#).

- [16] T. Sjostrand, S. Mrenna and P.Z. Skands, *PYTHIA 6.4 Physics and Manual*, *JHEP* **05** (2006) 026 [[hep-ph/0603175](#)].
- [17] E. Rutherford, *The scattering of α and β particles by matter and the structure of the atom*, *London Edinburgh Dublin Philos. Mag. & J. Sci.* **21** (1911) 669.
- [18] J. Chadwick, *The existence of a neutron*, *Proc. R. Soc. Lond. A* **136** (1932) 692.
- [19] P. Dirac, *The quantum theory of the electron*, *Proc. R. Soc. Lond. A* **117** (1928) 610.
- [20] C.D. Anderson, *The apparent existence of easily deflectable positives*, *Science* **76** (1932) 238.
- [21] M. Thomson, *Modern Particle Physics*, Cambridge University Press, Cambridge (Sept., 2013), [10.1017/CBO9781139525367](#).
- [22] Y. Ne’eman, *Derivation of strong interactions from a gauge invariance*, *Nucl. Phys.* **26** (1961) 222.
- [23] M. Gell-Mann, *Symmetries of baryons and mesons*, *Phys. Rev.* **125** (1962) 1067.
- [24] JADE collaboration, *Observation of Planar Three Jet Events in $e^+ e^-$ Annihilation and Evidence for Gluon Bremsstrahlung*, *Phys. Lett. B* **91** (1980) 142.
- [25] M.E. Peskin and D.V. Schroeder, *An Introduction to quantum field theory*, Addison-Wesley, Reading, USA (1995), [10.1201/9780429503559](#).
- [26] H.D. Politzer, *Asymptotic Freedom: An Approach to Strong Interactions*, *Phys. Rept.* **14** (1974) 129.
- [27] K. Hubner, *Design and construction of the ISR*, in *40th Anniversary of the First Proton-Proton Collisions in the CERN Intersecting Storage Rings (ISR)*, 6, 2012 [[1206.3948](#)].
- [28] S. Erhan, W.S. Lockman, T. Meyer, J. Rander, P. Schlein, R. Webb et al., *Hyperon production in pp interactions at $\sqrt{s} = 53$ and 62 GeV*, *Phys. Lett. B* **85** (1979) 447.
- [29] “Design Report Tevatron 1 project.”
<https://lss.fnal.gov/archive/design/fermilab-design-1984-01.pdf>, 1984.
- [30] D0 collaboration, *Observation of the top quark*, *Phys. Rev. Lett.* **74** (1995) 2632 [[hep-ex/9503003](#)].
- [31] CDF collaboration, *Observation of top quark production in $\bar{p}p$ collisions*, *Phys. Rev. Lett.* **74** (1995) 2626 [[hep-ex/9503002](#)].
- [32] L. Evans and P. Bryant, eds., *LHC Machine*, *JINST* **3** (2008) S08001.
- [33] CERN, “Atlas images gallery.”
<https://home.cern/resources/image/experiments/atlas-images-gallery>, 2011.